Microbial Pathogenesis 112 (2017) 38–49

Contents lists available at ScienceDirect

Microbial Pathogenesis

journal homepage: www.elsevier.com/locate/micpath

Inhibition of MEK-ERK1/2-MAP kinase signalling pathway reduces rabies virus induced pathologies in mouse model

Venkataravanappa Manjunatha [a, b], Karam Pal Singh [b, *], Mani Saminathan [a], Rajendra Singh [a], Nayakwadi Shivasharanappa [c], Channakeshava Sokke Umeshappa [d], Kuldeep Dhama [a], Gundallahalli Bayyappa Manjunathareddy [e]

[a] Division of Pathology, ICAR-Indian Veterinary Research Institute, Izatnagar, Bareilly, Uttar Pradesh, India
[b] Centre for Animal Disease Research and Diagnosis, ICAR-Indian Veterinary Research Institute, Izatnagar, Bareilly, Uttar Pradesh, India
[c] Animal Science Section, ICAR-Central Coastal Agricultural Research Institute, Ela, Goa, India
[d] Cancer Research Unit, Saskatchewan Cancer Agency, University of Saskatchewan, Saskatoon, Canada
[e] ICAR-National Institute of Veterinary Epidemiology and Disease Informatics, Bengaluru, Karnataka, India

ARTICLE INFO

Article history:
Received 20 June 2017
Received in revised form
18 September 2017
Accepted 18 September 2017
Available online 20 September 2017

Keywords:
U0126
MEK1/2 inhibitor
Rabies virus
Histopathology
Cytokines
T lymphocytes

ABSTRACT

The extracellular signal-regulated kinase (ERK) pathway has been shown to regulate pathogenesis of many viral infections, but its role during rabies virus (RV) infection *in vivo* is not clear. In the present study, we investigated the potential role of MEK-ERK1/2 signalling pathway in the pathogenesis of rabies in mouse model and its regulatory effects on pro-inflammatory cytokines and other mediators of immunity, and kinetics of immune cells. Mice were infected with 25 LD_{50} of challenge virus standard (CVS) strain of RV by intracerebral (i.c.) inoculation and were treated i.c. with U0126 (specific inhibitor of MEK1/2) at 10 μM/mouse at 0, 2, 4 and 6 days post-infection. Treatment with U0126 resulted in delayed disease development and clinical signs, increased survival time with lesser mortality than untreated mice. The better survival of inhibitor-treated and RV infected mice was positively correlated with reduced viral load and reduced viral spread in the brain as quantified by real-time PCR, direct fluorescent antibody test and immunohistochemistry. CVS-infected/mock-treated mice developed severe histopathological lesions with increased Fluoro-Jade B positive degenerating neurons in brain, which were associated with higher levels of serum nitric oxide, iNOS, TNF-α, and CXCL10 mRNA. Also CVS-infected/U0126-treated mice revealed significant decrease in caspase 3 but increase in Bcl-2 mRNA levels and less TUNEL positive apoptotic cells. CVS-infected/U0126-treated group also showed significant increase in $CD4^+$, $CD8^+$ T lymphocytes and NK cells in blood and spleen possibly due to less apoptosis of these cells. In conclusion, these data suggest that MEK-ERK1/2 signalling pathway play critical role in the pathogenesis of RV infection *in vivo* and opens up new avenues of therapeutics.

1. Introduction

Rabies is a progressive and zoonotic neurological disease of warm-blooded mammals including humans, caused by genus *Lyssavirus* and family *Rhabdoviridae* [1–3]. The clinical signs in dogs manifested as two different forms namely, furious form and dump form. Both the forms are dangerous and ultimately lead to death within 10 days of appearance of first clinical signs like change in behaviour and paralysis [3]. Mouse (3–4 weeks old or a litter of 2-day-old newborn mice) inoculation through intracerebral route is commonly used to study the pathogenesis of various rabies virus (RV) strains. The mouse model has various advantages like large amount of virus can be isolated from a brain,

List of abbreviations: CVS, challenge virus standard; DAB, 3,3'-Diaminobenzidine; dFAT, direct fluorescent antibody test; DPI, day post-infection; ERK, extracellular signal-regulated kinase; FACS, Fluorescence-activated cell sorting; FJB, Fluoro-Jade B; H&E, haematoxylin and eosin; HPI, hours post infection; i.c., intracerebrally; IHC, immunohistochemistry; IL, interleukin; iNOS, inducible nitric oxide synthase; MAPK, mitogen-activated protein kinase; NK, natural killer; NO, nitric oxide; PBMC, peripheral blood mononuclear cell; PBS, phosphate-buffered saline; qRT-PCR, quantitative real-time PCR; RV, rabies virus; RT, room temperature; TNF-α, tumour necrosis factor-α.

* Corresponding author. Pathology Laboratory, CADRAD, ICAR-Indian Veterinary Research Institute, Izatnagar, Bareilly, Uttar Pradesh, India.
E-mail address: karam.singh@rediffmail.com (K.P. Singh).

https://doi.org/10.1016/j.micpath.2017.09.044
0882-4010/

identification of RV strains, easily practicable, skills and facilities are not required, and histological examination of Negri bodies [3]. The mitogen-activated protein kinases (MAPKs) are important intermediates in signalling pathways that transduce extracellular signalling into intracellular responses. MAPKs include ERK 1 and 2, and MEK1/2 signalling pathways which plays important role in the regulation of cell survival, proliferation, differentiation and cell death [4,5]. Many viruses manipulate ERK-MAPK pathway for optimal viral replication [6–10]. The activation of ERK1/2–dependent signalling is a key process leading to selective induction of iNOS, TNF-α, IL-6, IL-8, metalloproteinases and CXCL10 transcription [11–13].

The U0126 (1,4-diamino-2,3-dicyano-1,4-bis[2-aminophenylthio]butadiene) is a potent and specific inhibitor of ERK signalling shown to inhibit MEK 1 and 2/MAPK 1 and 2, and inhibits pro-inflammatory cytokines [6,13,14]. Many viruses like human immunodeficiency virus-1 (HIV-1), herpes simplex virus type 1 (HSV-1), rabies virus [11,12], porcine reproductive and respiratory syndrome virus (PRRSV), coxsackievirus B3 [7], human astrovirus [9], influenza B virus [8,10], rhinovirus, herpes virus and Borna disease virus [6] activate MEK-ERK1/2 signalling pathway for their optimal replication of virus in host cells. Treatment with MEK1/2 inhibitor, U0126 significantly suppressed the post internalization step in viral replication process, including viral RNA synthesis, protein expression and virus production, and blocked the virus spread to neighbouring cells [6]. ERK1/2 activity might be necessary to phosphorylate or stabilize the viral RNA dependent RNA polymerase, which is essential for the initiation of viral RNA replication [7,9]. Rodríguez et al. [15] reported that U0126 inhibits multiplication of arenaviruses such as Junín, Pichinde and Tacaribe in human and monkey cell cultures by inhibiting Raf/MEK/ERK signalling pathway. Treatment with U0126 in VERO cells inhibits yellow fever virus induced ERK1/2 phosphorylation and replication by ~99% [16]. Treatment with U0126 reduced the levels of NS4AB and endoplasmic reticulum membrane invagination stimulation during the dengue virus (DENV-2 and -3) and Saint-Louis encephalitis virus infection. *In vivo* results showed that U0126 significantly reduced the yellow fever virus titers in brain of mice [16].

In vitro studies showed that RV activates ERK1/2-mediated signalling pathway, which stimulates macrophages resulted in secretion of various pro-inflammatory cytokines, including interferon (IFN)-α, IFN-β, interleukin (IL)-1α, IL-1β, IL-6, chemokines (CXCL10 and CCL5), nuclear factor κB (NF-κB) and NO [11,12]. Chemokines have been associated with variety of neurodegenerative disorders [17]. Nitric oxide is not normally detectable in brain, but detectable after RV infection and peroxynitrites caused oxidative injury to neurons leading to neuronal dysfunction [18,19]. Treatment with ERK1/2 inhibitors such as U0126 reduced the RV induced NO, iNOS and CXCL10 production.

Although several *in vitro* studies have reported the role of MEK-ERK1/2 pathway in rabies infection [11,12], its role in rabies pathogenesis is not yet tested in clinically relevant *in vivo* model. In the present study, treatment with U0126 resulted in delayed development of clinical signs, increased survival time and lower incidence of disease in mice than CVS-infected/mock-treated. Treatment also reduced viral load and mitigated viral spread in the brain. CVS-infected/mock-treated mice developed severe histopathological lesions with higher levels of serum nitric oxide, iNOS, TNF-α, and CXCL10 mRNA expression in brain. Inhibition of MEK1/2 signalling significantly increased $CD4^+$, $CD8^+$ T lymphocytes and NK cells in blood and spleen. The results confirm the crucial role of MEK-ERK1/2 signalling pathway in the pathogenesis of RABV infection *in vivo*.

2. Materials and methods

2.1. Mice and ethical statement

Young Swiss albino mice (2–3 weeks age) of either sex were procured from Laboratory Animal Resource (LAR) Section of the Institute. The mice were kept in polypropylene cages and provided feed and water ad libitum. The animals were kept under controlled conditions (temperature 27 ± 2 °C; relative humidity 30–55%) with 12/12 h light/dark cycle. All the experiments were carried out as per the prescribed guidelines of the Institute Animal Ethics Committee (IAEC).

2.2. Virus and U0126

The CVS strain of rabies virus was provided by Division of Biological Products, ICAR-IVRI, Izatnagar. The virus dose was calculated by mouse inoculation test (MIT) using Reed and Muench method. After determining LD_{50} titre, the virus aliquots were stored at −80 °C. The MEK inhibitor, U0124 was dissolved in dimethyl sulfoxide (DMSO) leading to final concentration of 10 μM U0126 solution and stored as frozen stocks at −20 °C.

2.3. Reagents and antibodies

Chemical inhibitor, U0126 and fluorescein isothiocyanate (FITC)-conjugated monoclonal antibodies specific for RV nucleoprotein were obtained from Sigma-Aldrich, St. Louis, USA. Other reagents Fluoro-Jade B stain (Merck Millipore, USA), RNAlater® (Qiagen), TRI Reagent® (Sigma-Aldrich, USA), Histopaque® (Sigma-Aldrich, USA), DeadEnd™ Colorimetric TUNEL System (Promega, Madison, USA), VECTASTAIN® ABC kit (Vector Laboratories, CA, USA) and total nitric oxide assay kit (cat no. EMSNOTOT, Pierce Biotech, USA) were procured from standard company. ELISA kit for estimation of phosphorylated (Thr202/Tyr204) and total ERK1/2 protein was purchased from Abcam, Cambridge, United Kingdom. Monoclonal antibodies like Mouse T Lymphocyte Subset Antibody Cocktail; PE-Cy7 CD3e, PE CD4, and FITC CD8a (Cat no. 558391) and PE-Cy™ 7 Mouse Anti-Mouse NK-1.1 antibody (Cat no. 552878) was procured from BD Pharmingen™, BD Biosciences, CA, USA.

2.4. Experimental intracerebral infection and drug treatment

After acclimatization, mice were divided into 4 groups. For intracerebral injection, the animal was grasped firmly by the loose skin behind the head at lateral side of hemisphere from midline. The skin was pulled taut and 26 gauge hypodermic needle was inserted perpendicularly through the skull into the brain and 0.01 mL of solution was injected. The site of injection was 2 mm from either side of the midline on a line drawn through the anterior base of the ears [20]. The i.c. injection procedure was approved by IAEC. Group-I (CVS-infected/mock treated, n = 28) mice were inoculated intracerebrally (i.c.) with 10 μl of 25 LD_{50} CVS strain of RV on day 0 and treated with 10 μl of DMSO alone (mock treated) on 0, 2, 4 and 6 DPI. The 25 LD_{50} dose of CVS strain of RV produced sufficient pathology in mouse model. Group-II (CVS-infected/U0126-treated, n = 28) mice were inoculated i.c. with 10 μl of 25 LD_{50} CVS on day 0 and treated with 10 μl of 10 μM U0126 (MEK1/2 inhibitor) per mouse on 0, 2, 4 and 6 DPI. Group-III (U0126 and DMSO-treated, n = 28) mice were inoculated i.c. with 10 μl each of 10 μM U0126 alone DMSO on 0, 2, 4 and 6 DPI. Group-IV (PBS-injected, n = 28) mice were inoculated i.c. with 10 μl of sterile phosphate-buffered saline (PBS) alone on 0, 2, 4 and 6 DPI. Three mice from each group were euthanized at 6, 12 and 24 h post infection (HPI), 5, 8 and 13 DPI by cervical dislocation.

2.5. Assessment of clinical signs and sample collection

The mice were observed for clinical signs, such as ruffled fur, tremors, hunchback appearance, in-coordination of hind limbs, paralysis and prostration till 13 DPI. Disease progression was evaluated by scoring the clinical signs as follows: 0 - normal mice; 1 - ruffled fur; 2 - tremors; 3 - incoordination; 4 - paralysis; 5 - prostration; and 6 - death [21]. During euthanasia blood was collected from heart with or without EDTA in vacutainers for serum and $CD4^+$, $CD8^+$ T lymphocytes and NK cells estimation by FACS. The serum was stored at −20 °C for estimation of nitric oxide [19]. The spleen was collected in ice for estimation of $CD4^+$, $CD8^+$ and NK cells. Tissues like brain, spleen, liver, kidney, lungs and heart were collected in 10% neutral buffered formalin for histopathology. Brain was collected in RNAlater® and stored in −20 °C for virus identification and estimation of various cytokines.

2.6. Histopathology

The coronal sections at the mid level of cerebrum, cerebellum and hippocampus were processed by paraffin embedding technique to obtain 4 μ thick sections and stained by haematoxylin and eosin (H&E). The lesions were scored in cerebrum, grey matter (3 laminae), white matter and hippocampus based on severity on a 0–3 scale (0 - normal histological architecture; 1 - mild meningitis, congestion/haemorrhage, neuronal degeneration, neural oedema and mild perivascular cuffing; 2 - moderate meningitis, congestion/haemorrhage, neuronal degeneration, gliosis, moderate perivascular cuffing and nonsuppurative encephalitis; 3 - severe meningitis, congestion/haemorrhage, neuronal degeneration, perivascular cuffing and nonsuppurative encephalitis).

2.7. Estimation of ERK1/2 kinase activity by ELISA

The amounts of phosphorylated (Thr202/Tyr204) and total ERK1/2 protein in brain was estimated by using commercially available ELISA kit (Abcam, Cambridge, United Kingdom) according to the manufacturer's instruction. The sensitivity of the kit for phospho-ERK is 0.1 ng/mL (range: 0.2–20 ng/mL) and total ERK1/2 is 0.6 ng/mL (range: 0.6–60 ng/mL). The phosphorylated ERK1/2 assay detects endogenous levels of ERK1/2 in tissue homogenate, only when phosphorylated at Thr202/Tyr204. Brain tissues were thoroughly washed with PBS to remove blood. 100–200 mg of tissue was minced and homogenized in chilled 1x cell extraction buffer (Abcam, Cambridge, United Kingdom). The mince was incubated for 20 min in ice and centrifuged at 18,000 × g for 20 min at 4 °C. Supernatants were collected in clean tubes and stored at −80 °C. The protein concentration in the sample was quantified by the Lowry method, using bovine serum albumin (BSA) as standard [22]. Samples were diluted to desired concentration (1–2 mg/mL) in 1x cell extraction buffer. Absorbance was measured at 405 nm using an ELISA plate reader and the concentrations of phosphorylated and total ERK1/2 proteins were calculated from the standard curve.

2.8. Direct fluorescent antibody test

The cryosections as well as smears prepared from cut sections of the brains were air dried, heat fixed and covered with 50 μl of anti-rabies nucleocapsid FITC conjugate. Slides were incubated at 37 °C for 1 h in a dark moist chamber and washed thrice with PBS (pH 7.2) and mounted with aqueous mountant. Finally, slides were viewed under fluorescent microscope (Leitz Leica, Germany) for the presence of specific apple green fluorescence. During the process, positive and negative controls were kept along with test slides.

2.9. Immunohistochemistry (IHC)

The paraffin sections were deparaffinised, rehydrated and microwaved in 10 mM tri-sodium citrate buffer (pH 6.0) for antigen retrieval [19]. Endogenous peroxidase activity was quenched with 0.3% hydrogen peroxide (H_2O_2) in methanol and blocked with 5% goat serum. Sections were incubated with primary anti-rabies monoclonal antibody for overnight at 4 °C in humidified chamber and biotinylated anti-mouse secondary antibody and VECTASTAIN ABC reagent (Vector Biologicals, USA) for 30 min at RT. Sections were stained with 3,3′-Diaminobenzidine (DAB) chromogen and counter-stained with Meyer's haematoxylin and mounted in aqueous medium. The distribution and intensity of positive signals were visualized under the light microscope. Quantitative analysis of immunopositive cells was done by counting both positive and negative cells (minimum of 1000 cells) in 15–20 representative high-power fields [19].

2.10. Peripheral blood mononuclear cell (PBMC) isolation

Anti-coagulated blood (approx. 0.5 mL from 3 mice) was pooled according to experimental groups and diluted with Dulbecco's PBS (D-PBS; 1x; pH 7.2; ratio 1:1) without calcium and magnesium. The diluted blood was subjected to density gradient separation by gentle layering of Histopaque® with density of 1.083 g/mL (ratio 1:1) and centrifuged at 1800 rpm for 10 min at RT which resulted in the separation of PBMCs at the plasma-histopaque interface. The PBMC layer was collected and washed in isotonic PBS (250 g for 10 min) and re-suspended in RPMI-1640 (Hyclone, Fischer Scientific, USA) for cell count and viability assay, and in Stain Buffer (BSA; BD Biosciences, USA) for flow cytometry. The cell viability was determined immediately by using trypan blue dye exclusion with PBS as the diluent. The cell viability was more than 90%.

2.11. Separation of splenocytes

Spleen was minced into small pieces and splenocytes were squeezed from the splenic capsule in PBS (pH 7.4) through 70 μm nylon mesh cell strainer in a Petri dish to create single cell suspension by gently mashing spleen pieces with the rubber end of a plunger from a 1 mL tuberculin syringe. Any large aggregates and tissue pieces were discarded. The suspensions of dispersed cells were again filtered through cell strainer into a sterile centrifuge tube on ice. Then, cells were centrifuged at 1500 rpm for 10 min at 4 °C and supernatant was discarded. The cell pellet was re-suspended in chilled red blood cell (RBC) lysis buffer and centrifuged at 1500 rpm for 5 min at 4 °C. Supernatant was discarded and pellet was washed in isotonic PBS (250 g for 10 min) and re-suspended in RPMI-1640 for cell count and viability assay, and in Stain Buffer (BSA; BD Biosciences, USA) for flow cytometry. The cell viability was determined immediately by using trypan blue dye exclusion with PBS as the diluent. The cell viability was more than 90%.

2.12. Flow cytometry

Cells isolated from blood and spleen were reconstituted in 200 μl of Stain buffer and processed for estimation of frequency of $CD4^+$, $CD8^+$ and NK cells by fluorescence-activated cell sorting (FACS) in various groups (BD FACSCalibur™ Instrument, USA). The cells were incubated with 10 μl of PE and FITC labelled cocktail antibody for CD4 and CD8 cells, respectively and 10 μl of PE-Cy 7 antibody for NK cells at RT in dark for 45 min. Ten thousand cells were counted during FACS and analysis of cells were performed using the BD CellQuest™ pro software (BD Bioscience, USA).

2.13. RNA extraction and reverse transcription

Total RNA was isolated from the brain by using TRIZOL reagent. The integrity of the RNA was tested by electrophoresis and reverse transcription was performed as per Baloul et al. [21]. Rabies virus nucleoprotein (RVN) gene was detected by reverse transcription with 1 μM RVN-protein-specific sense primer instead of oligo dT.

2.14. Quantitative real-time PCR (qRT-PCR)

Chemokine CXCL10, cytokine TNF-α and other molecules like iNOS, caspase-1 and Bcl-2 mRNA expression (relative quantification), and rabies viral genome quantification (absolute quantification) in brain samples were carried out by qRT-PCR (Mx 3000TM System, Stratagene, USA), using SYBR Green 1 dye and gene specific primers mentioned in Table 1. The PCR reactions were set up with 25 μl reaction mix consisting of 10 μl of 2.5X QuantiTech SYBR Green PCR master mix, 1 μl (10 pmol) of each gene-specific primer and 2 μl of cDNA template (100 ng concentration). Cytokine/chemokine gene expression was measured by quantification of the cDNA with respect to the cDNA from uninfected mice as a calibrator. All quantifications were normalised with respect to an endogenous control β-actin. The relative value obtained for quantification was expressed as $2^{-\Delta\Delta Ct}$ [19].

For absolute quantification of rabies viral RNAs, a standard curve was generated using serial dilutions of known rabies-specific DNA copy numbers (PCR product) by running test samples in qRT-PCR. An absolute standard curve method was used to calculate the copy numbers of RV N RNA in mouse brain tissue. To exclude the contamination of genomic DNA, control cDNA reactions were prepared in parallel without reverse transcriptase. These were uniformly negative.

2.15. Estimation of total nitric oxide in serum

Serum samples collected from different groups at various time intervals were subjected to total nitric oxide estimation by Griess reaction. Briefly, 200 μl of 1x reagent diluent was pipetted into duplicate wells in a 96-well-plate. Then 50 μl of diluted nitrate standard and samples were added followed by 25 μl of NADH and diluted nitrate reductase and plates were incubated at 37 °C for 30 min. Later, 50 μl of Griess reagent I followed by 50 μl of Griess reagent II were added to all the wells, and incubated at room temperature (RT) for 10 min. Optical density (OD) of each well was taken using a micro-plate reader at 550 nm wavelength.

2.16. Fluoro-Jade B staining

The brain sections were mounted on 2% gelatine coated slides and immersed in 1% sodium hydroxide (NaOH) in 80% alcohol (20 mL of 5% NaOH added to 80 mL absolute alcohol) for 5 min, followed by 70% alcohol for 2 min and in distilled water for 2 min. The slides were incubated with 0.06% potassium permanganate for 10 min and stained with 0.0004% FJB for 20 min. The slides were cleared by immersion in xylene for 1 min before mounting with DPX. FJB labelled degenerating neurons were visualized under ultra-violet illumination [27].

2.17. TUNEL staining for detection of apoptosis

The brain sections were fixed in 4% para-formaldehyde and permeabilized by proteinase K (20 μg/mL). They were equilibrated with equilibration buffer and incubated with rTdT reaction mix for 60 min in humidified chamber. The reaction was terminated with 2x SSC. The endogenous peroxidase was blocked with 0.3% H_2O_2 and incubated with streptavidin HRP (1:500). DAB chromogen was added for colour development and slides were mounted. Apoptotic cells were observed under light microscope. Quantitative analysis of TUNEL positive cells was done by counting both positive and negative cells (minimum of 1000 cells) in 5–10 representative high-power fields [19].

2.18. Statistical analysis

Statistical analysis was performed using GraphPad Prism version 4.0 software (San Diego, California, USA). The one-way ANOVA followed by Tukey's Post-hoc test was used to analyze the data from different groups in respect of various parameters. The P value < 0.05 was considered statistically significant difference between the control and treated groups.

3. Results

3.1. Clinical signs and survival rate

Progression of the disease was assessed by mean clinical score (Fig. 1a). In CVS-infected/mock-treated group, clinical signs had developed on 3 DPI, became severe on 5 DPI onwards and all the mice died on 9 DPI. The maximum intensity of clinical signs and mortality was observed on 8 and 9 DPI (Fig. 2). The mice had ruffled fur (3 mice) and tremors (3 mice) on 5 DPI. There were incoordination and paralysis (5 mice) on 6 DPI, and prostration (7

Table 1
Primers used for amplification of different genes by conventional PCR and real-time PCR.

Gene name	Primer sequences	Annealing temperature	Product size (bp)	References
RabN	F:5′-AATCAGGTGGTCTCTTTGAAG-3′ R:5′-AGCCCAATTCCCTTCTACATC-3′	50	329	Self designed
RabN	F:5′-TATGAGTACAAGTACCCTGCC-3′ R:5′-ATTCCATAGCTGGTCCAGTCTTC-3′	50	205	Self designed
β-actin/P/M	F:5′-TCTAGGCACCAAGGTGTG-3′ R:5′-TCATGAGGTAGTCCGTCAGG-3′	56	460	Mckimmie et al. [23]
CXCL10	F:5′-CACCATGAACCCAAGTGCTGCCGT-3′ R:5′-AGGAGCCCTTTTAGACCTTTTTTG-3′	55	297	Nagpal et al. [24]
TNF-α	F:5′-CCCTTTACTCTGACCCCTTT-3′ R:5′-AACCTGACCACTCTCCCTTT-3′	62	310	Mckimmie et al. [23]
iNOS/P2/M	F:5′-TGCATGGACCAGTATAAGGCAAGC-3′ R:5′-CTCCTGCCCACTGAGTTCGTC-3′	55	288	Doi et al. [25]
Caspase 3	F:5′-GGCTTGCCAGAAGATACCGGT-3′ R:5′-GCATAAATTCTAGCTTGTGCGCGTA-3′	55	150	Mckimmie et al. [23]
Bcl2	F:5′- GATGACTTCTCTCGTCGCTAC-3′ R:5′-ACGCTCTCCACACACATGAC-3′	56	182	Shams et al. [26]

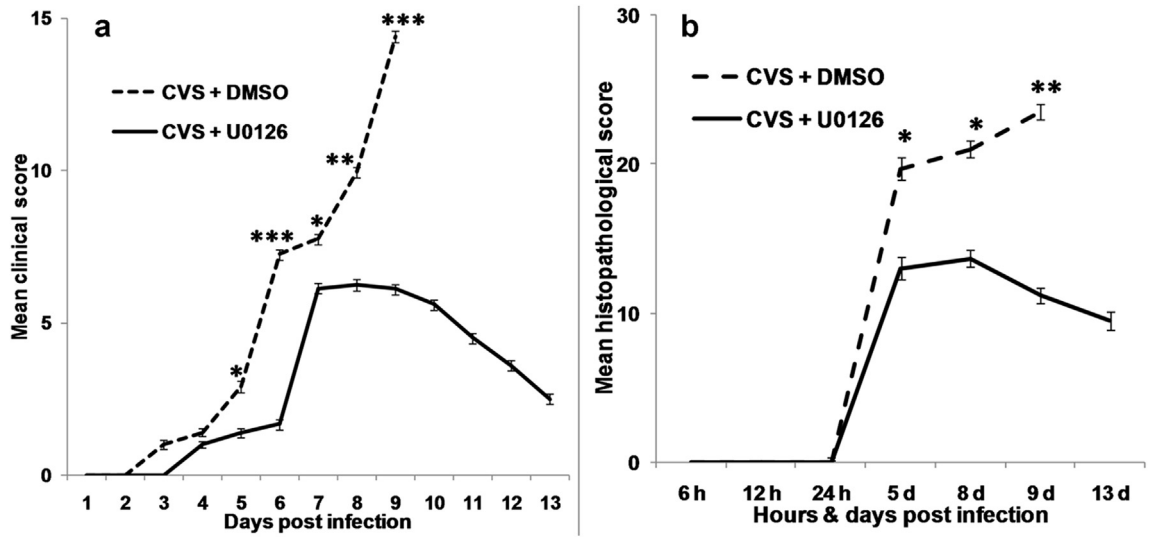

Fig. 1. Mean clinical (a) and histopathological (b) score in CVS-infected/mock-treated (dotted line) and MEK-ERK1/2 inhibited (solid line) groups (n = 28 mice/group). Mean with asterisks (*P < 0.05; **p < 0.001; ***p < 0.0001) at a given DPI indicates statistically significant. Error bars indicate the SD.

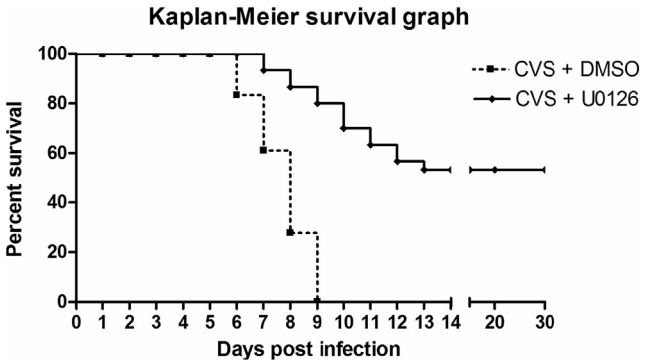

Fig. 2. Kaplan–Meier survival curve for CVS-infected/mock-treated (dotted line) and MEK-ERK1/2 inhibited (solid line) groups (n = 18 mice/group) and mortality was recorded daily.

mice) on 7 DPI. All mice in this group were dead by 9 DPI (Fig. 2). Strikingly, in CVS-infected/U0126-treated group mice exhibited less severe clinical signs even on 6 DPI with less number of animals were affected, and mortality was started on 7 DPI and 50% of mice were survived much longer. After 13 DPI, 4 mice were survived up to 30 DPI and were euthanized (Fig. 2). The other two groups of mice (U0126 alone and PBS alone) were found to be normal throughout the experiment.

3.2. Gross lesions and histopathology

The CVS-infected/mock-treated mice showed severe meningeal congestion in brain, debility, marked reduction in spleen size, and distention of urinary bladder. However, these changes were milder in CVS-infected/U0126-treated group. The inhibitor control and negative control groups had no changes throughout the experimental period. The severity of histopathological lesions was assessed by mean histopathological score (Fig. 1b). On 5 DPI, CVS-infected/mock-treated group showed characteristic perivascular infiltration of mononuclear cells (MNCs) in the grey and white matter, mild meningitis, pyknotic neurons with acidophilic cytoplasm and foci of glial nodules in cerebral hemisphere (Fig. 3a). The neurons of dentate gyri and CA2 regions were degenerated with mild diffuse microgliosis. However, The CVS-infected/U0126-treated group had less severe lesions (Fig. 3b). On 8 and 9 DPI, CVS-infected/mock-treated group showed severe neuronal changes like pyknotic neurons and karyorrhexis in cerebral hemisphere and hippocampus (CA1 and CA2 regions), and CVS-infected/U0126-treated group merely showed mild perivascular reaction and gliosis. On 13 DPI, MAP kinase treated group had more mild reaction like sparse infiltration of MNCs in meninges and mild neuronal degeneration in CA2 region. Overall, lesions were more prominent in cerebrum and hippocampus in brain than other anatomical sites. Histopathological changes were not seen in the brains of control groups mice (Fig. 3c and d).

3.3. Estimation of ERK1/2 kinase activity

The CVS-infected/mock-treated mice had higher levels of phosphorylated (pT202/Y204) and total ERK1/2 at 12 HPI onwards, which reached peak on 8 DPI in brain homogenates. The CVS-infected/U0126-treated mice had lower levels of phosphorylated (Fig. 4a) and total (Fig. 4b) ERK1/2. No significant variations were noticed in control mice.

3.4. Quantification of viral load

Rabies viral nucleoprotein (N gene) was detected in brain samples as early as at 6 HPI. During 6 and 24 h post infection, the number of copies was higher in CVS-infected/mock-treated group than in CVS-infected/U0126-treated mice. Strikingly, the viral load was very significantly low in CVS-infected/U0126-treated group at 8 and 9 DPI. On 13 DPI, the virus concentration was drastically reduced in CVS-infected/U0126-treated group over the course of infection (Table 2).

3.5. dFAT and IHC

The rabies virus infected brain sections revealed weak positive signals with dFAT up to 24 HPI with specific apple green fluorescence. The signals were more intense at subsequent time intervals in CVS-infected/mock-treated group (Fig. 5a) than in CVS-infected/U0126-treated group (Fig. 5b). In IHC, immunopositive brown signals were more intense and significantly higher number of neurons

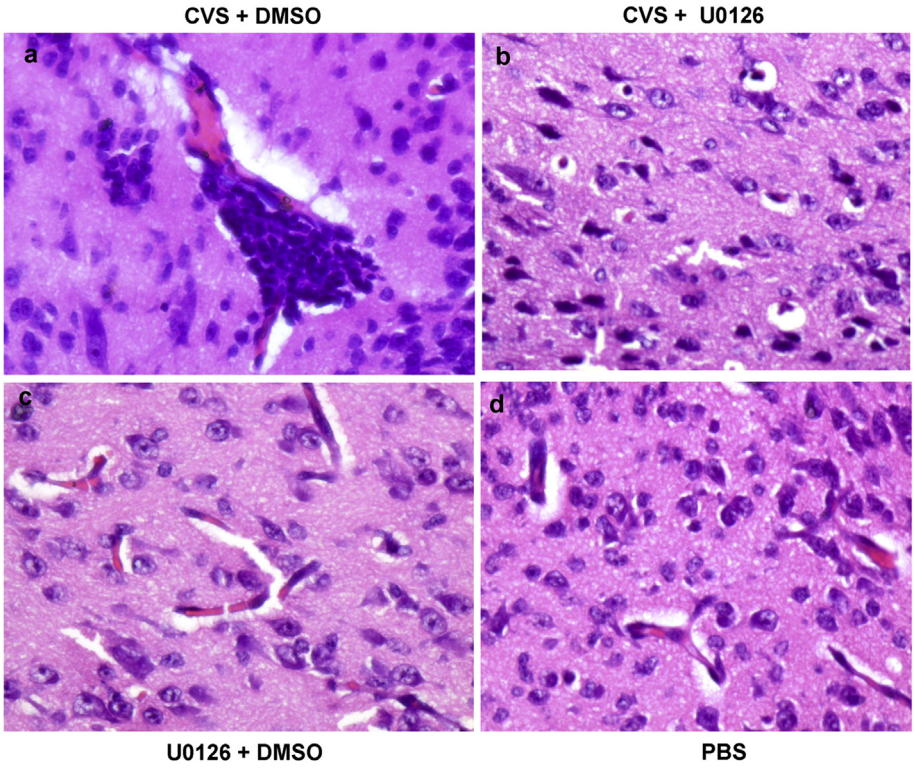

Fig. 3. Histopathological findings on 8 DPI in different groups. **a.** Perivascular infiltration of mononuclear cells, severe edema and neuronal degeneration in cerebral cortex of CVS-infected/mock-treated group. H&E x400. **b.** Mild perivascular edema and mild neuronal degeneration in cerebral cortex of MEK-ERK1/2 inhibited groups. H&E x400. **c and d.** Normal histology of brain in inhibitor (U0126) control (c) and negative (PBS) control (d) groups. H&E x400.

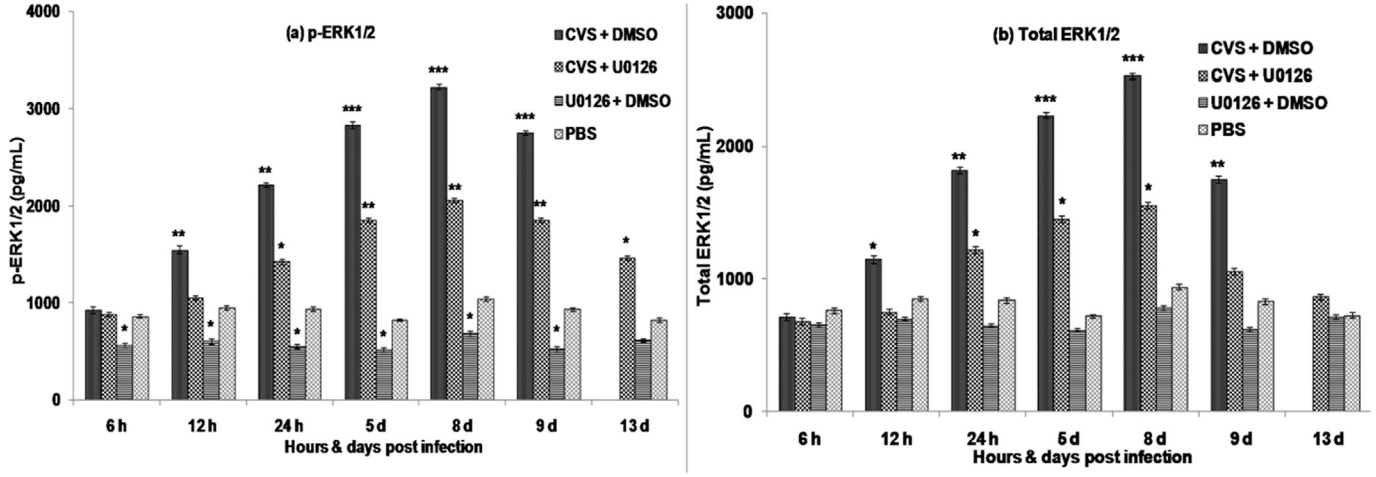

Fig. 4. a. Phosphorylated ERK1/2 (pT202/Y204) and **b.** total ERK1/2 levels (pg/mL) in brain homogenate of various groups (n = 28 mice/group). Mean with asterisks (*P < 0.05; **p < 0.001; ***p < 0.0001) at a given DPI indicates statistically significant when compared to PBS control. Error bars indicate the SD.

Table 2
Absolute copy number of rabies virus in CVS-infected/mock-treated, and CVS-infected/U0126-treated groups by real-time PCR.

Hours and days post infection	Group-I (CVS + DMSO)	Group-II (CVS + U0126)
6 h	1.69×10^4	1.03×10^4
12 h	1.97×10^4	1.21×10^4
24 h	1.91×10^5	$1.58 \times 10^{4*}$
5 d	1.09×10^{10}	$4.86 \times 10^{8*}$
8 d	1.69×10^{10}	$1.05 \times 10^{8*}$
9 d	1.76×10^{10}	$1.42 \times 10^{6*}$
13 d	–	3.58×10^4

The mean with asterisks (*) at a given HPI and DPI indicates statistically significant (P < 0.05) when compared to group-I.

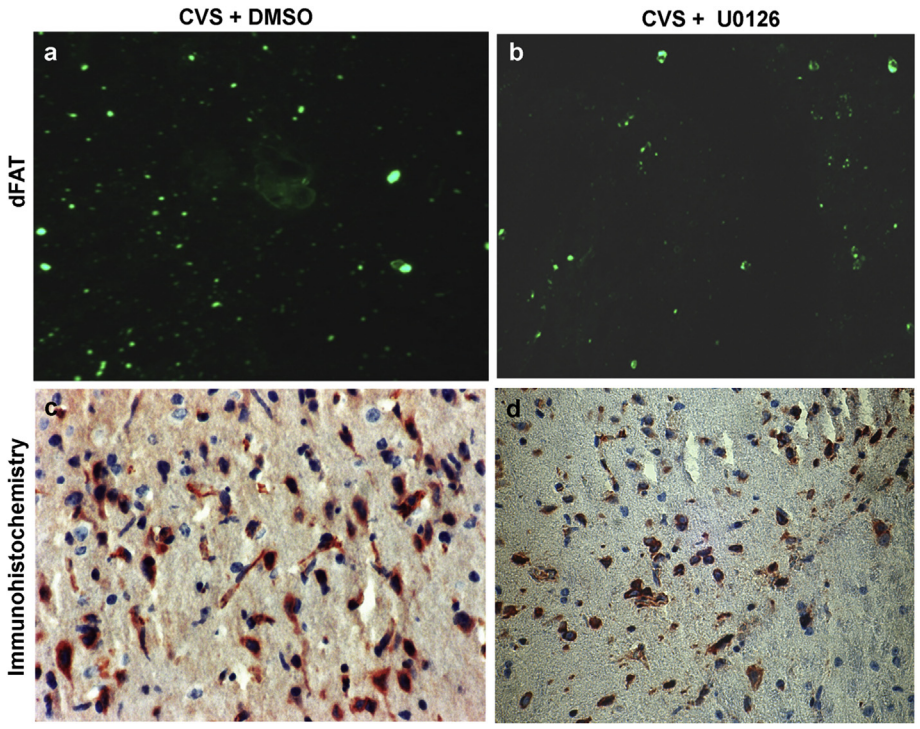

Fig. 5. Direct fluorescent antibody technique (dFAT) and immunohistochemical detection of rabies virus in CVS-infected/mock-treated (a, c) and MEK-ERK1/2 inhibited (b, d) groups. **a.** Brain showing strong and diffuse positive signals with bright apple green fluorescence of rabies antigen in brain. dFAT x200. **b.** MEK-ERK1/2 inhibited mice brain showing mild and weak positive signals. dFAT x200. **c.** Cerebral cortex showing strong positive signals for rabies antigen in neuronal cytoplasm. IHC-DAB-MH x200. **d.** Cerebral cortex showing weak positive signals of rabies antigen. IHC-DAB-MH x200. (For interpretation of the references to colour in this figure legend, the reader is referred to the web version of this article.)

showed positive signals in cerebrum of CVS-infected/mock-treated mice (Fig. 5c) than in CVS-infected/U0126-treated mice, which showed mild signals and less number of positive neurons (Fig. 5d). On 5, 8, 9 and 13 DPI, cerebral cortex and hippocampus showed more positive signals than cerebellum. The quantification of immunopositive neurons in brain of CVS-infected/mock-treated and CVS-infected/U0126-treated groups has been presented in Fig. 6a.

3.6. Kinetics of immune cell population (immunophenotyping)

Both infected groups (I and II) showed significantly increased number of $CD4^+$ and $CD8^+$ T cells in blood and spleen up to 24 HPI than in control groups (Fig. 7a and b). From 5 to 13 DPI the numbers of $CD4^+$ and $CD8^+$ T cells were lower in CVS-infected/mock-treated mice. However, the decline was lower in CVS-infected/U0126-treated group (Fig. 7). On 8 DPI, the levels of $CD4^+$ and $CD8^+$ T

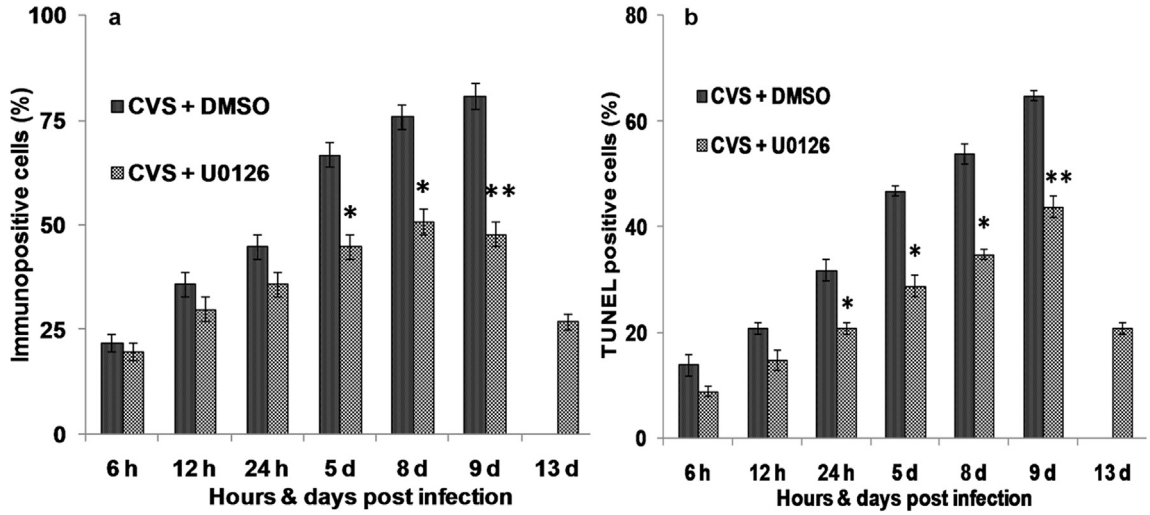

Fig. 6. Quantification of immunopositive (a) and TUNEL positive (b) cells in brain parenchyma in CVS-infected/mock-treated and MEK-ERK1/2 inhibited groups (n = 28 mice/group). Mean with *P < 0.05; **p < 0.001 indicates statistically significant. Error bars indicate the SD.

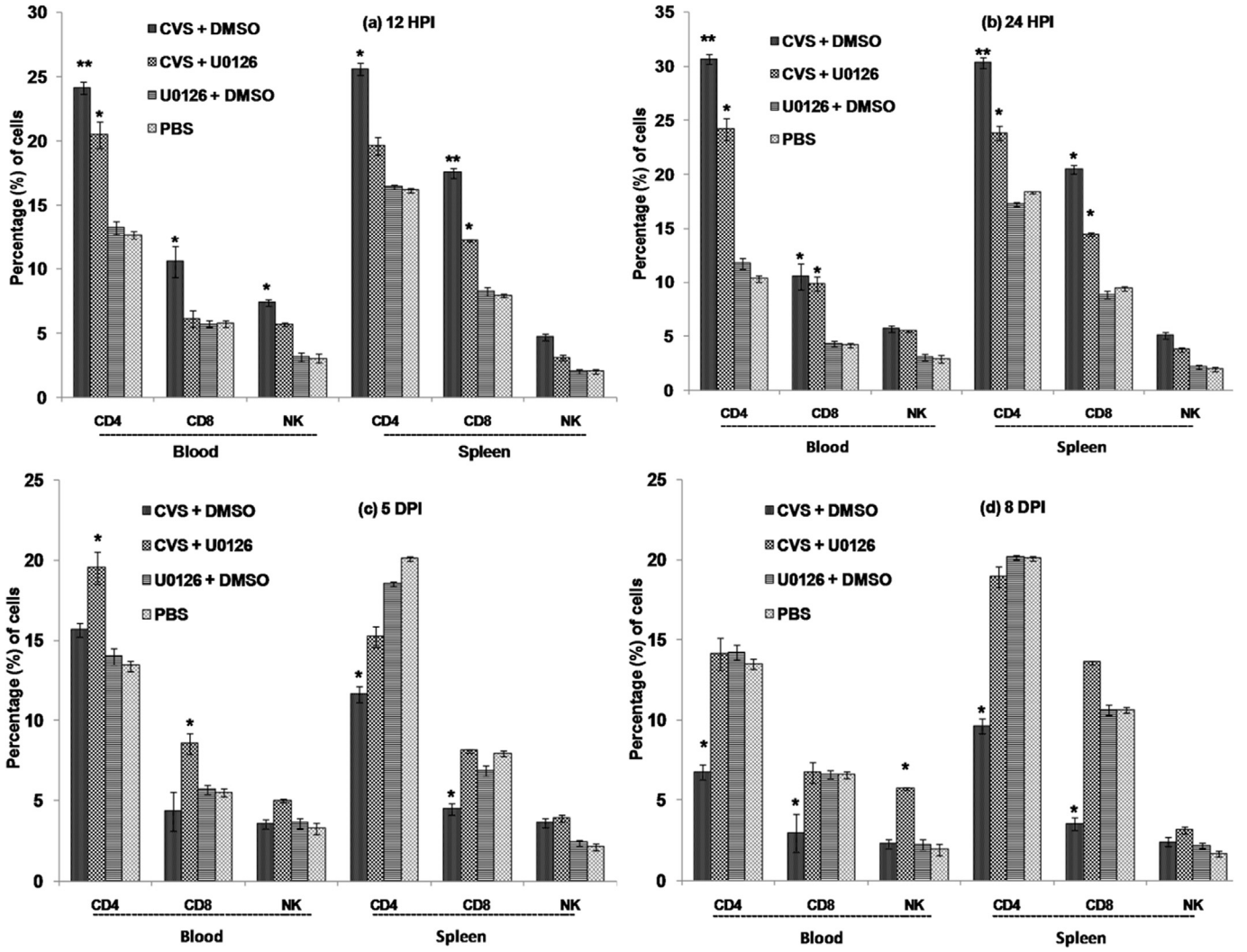

Fig. 7. Kinetics of immune cell population in blood and spleen of various groups at different days post infection (DPI). Mean with asterisks (*P < 0.05; **p < 0.001) at a given DPI indicates statistically significant when compared to PBS control. Error bars indicate the SD.

cells in blood and spleen were significantly low in CVS-infected/mock-treated than CVS-infected/U0126-treated group (Fig. 7d). In blood the $CD4^+/CD8^+$ ratio in CVS-infected/mock-treated mice increased till 8 DPI and then gradually decreased. But the pattern was reverse in CVS-infected/U0126-treated group. In spleen the ratios in both groups revealed opposite trend compared to blood (data not shown).The NK cells also followed the similar kinetics as $CD4^+$ and $CD8^+$ T cells (Fig. 7).

3.7. qPCR for CXCL10, TNF-α, iNOS, caspase 3 and Bcl-2 mRNA expression

The *CXCL10*, TNF-α and *iNOS* mRNA expressions were significantly higher and reached peak on 8 and 9 DPI in CVS-infected/mock-treated group as compared to CVS-infected/U0126-treated group (Fig. 8a,b,c). Consistently, the nitric oxide levels in serum were found to be higher in CVS-infected/mock-treated mice (Fig. 8d). Interestingly, the caspase 3 mRNA expression was up regulated as early as 6 HPI, and reached peak on 9 DPI in CVS-infected/mock-treated group when compared to CVS-infected/U0126-treated group, which had revealed significantly low levels at all intervals (Fig. 8f). The Bcl-2 mRNA expression did not vary in all the groups up to 12 HPI, but expression was increased at 24 HPI, significantly high at 5 DPI, and highest on 13 DPI in CVS-infected/U0126-treated group (Fig. 8e). The CVS-infected/mock-treated group showed lower levels at all intervals. The *CXCL10*, TNF-α, *iNOS*, caspase 3 and Bcl-2 mRNA expression in both the control groups were not affected.

3.8. Fluoro-Jade B staining

Brain sections of both infected group (I and II) mice did not show any FJB positive degenerating neurons with specific bright green fluorescence at 6, 12 and 24 HPI. On 5 DPI, CVS-infected/mock-treated group showed few FJB positive neurons. Later, greater number of FJB positive neurons was found in cerebral cortex, hippocampus and cerebellum on 8 DPI (Fig. 9a), in comparison to a few in CVS-infected/U0126-treated group (Fig. 9b). On 13 DPI, CVS-infected/U0126-treated group showed few FJB positive neurons in all parts of brain. The brain sections from control mice were negative for FJB positive neurons.

3.9. TUNEL assay and DNA ladder pattern

Consistent with higher expression of caspase 3 mRNA, TUNEL positive apoptotic cells were widespread in brain, especially in

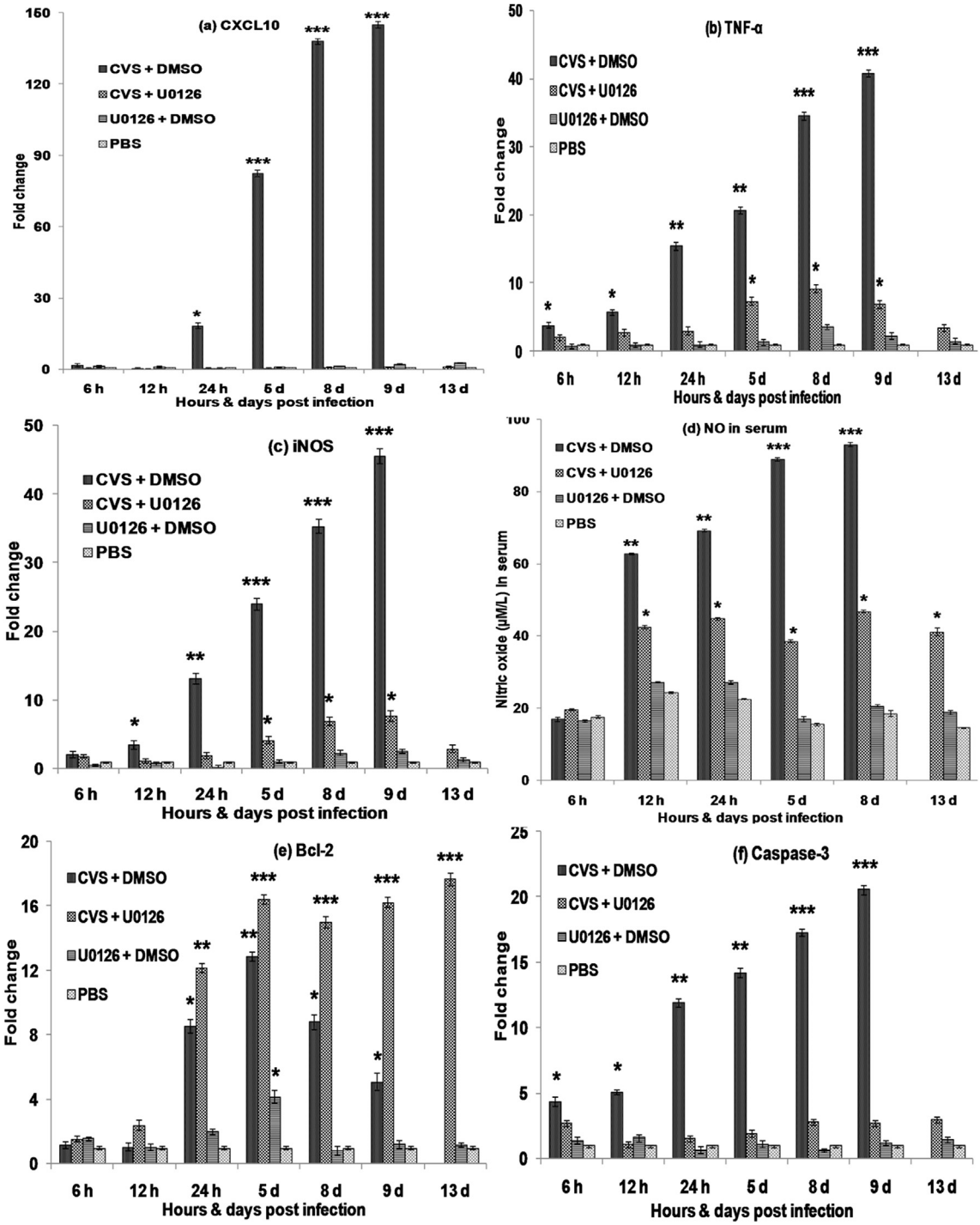

Fig. 8. Relative expression profiles of different genes (a,b,c,e,f) in brain by quantitative real-time PCR and nitric oxide (μM/L) in serum (d) from various groups. Relative expression of genomic mRNA was calculated as $2^{-\Delta\Delta Ct}$ and compared to non-infected mice. The mean with asterisks (*P < 0.05; **p < 0.001; ***p < 0.0001) at a given DPI differs significantly when compared to PBS control. Error bars indicate the SD.

hippocampus and cerebral cortex in the CVS-infected/mock-treated group (Fig. 9c). However, in CVS-infected/U0126-treated group mice showed only a few TUNEL positive cells (Fig. 9d). Apoptotic cells in the CVS-infected/mock-treated brain sections could be detected as early as 24 HPI and were abundant on 8 and 9 DPI (Fig. 6b). These results were also confirmed by DNA ladder assay and typical ladder pattern of 200 bp size was seen in CVS-infected/mock-treated group, but CVS-infected/U0126-treated group did not show typical ladder pattern (data not shown).

4. Discussion

To better understand the role of MEK-ERK1/2-MAPK signalling pathway in pathogenesis of rabies and its inhibitory effect on pro-inflammatory cytokines (CXCL10, TNF-α), iNOS and other molecules (caspase-3 and Bcl-2), the present study was conducted. Use of MEK-ERK-1/2 inhibitors did delay in development of clinical signs, increased survival rate and duration. The delay in commencement of clinical signs and better survivability of mice could be due to

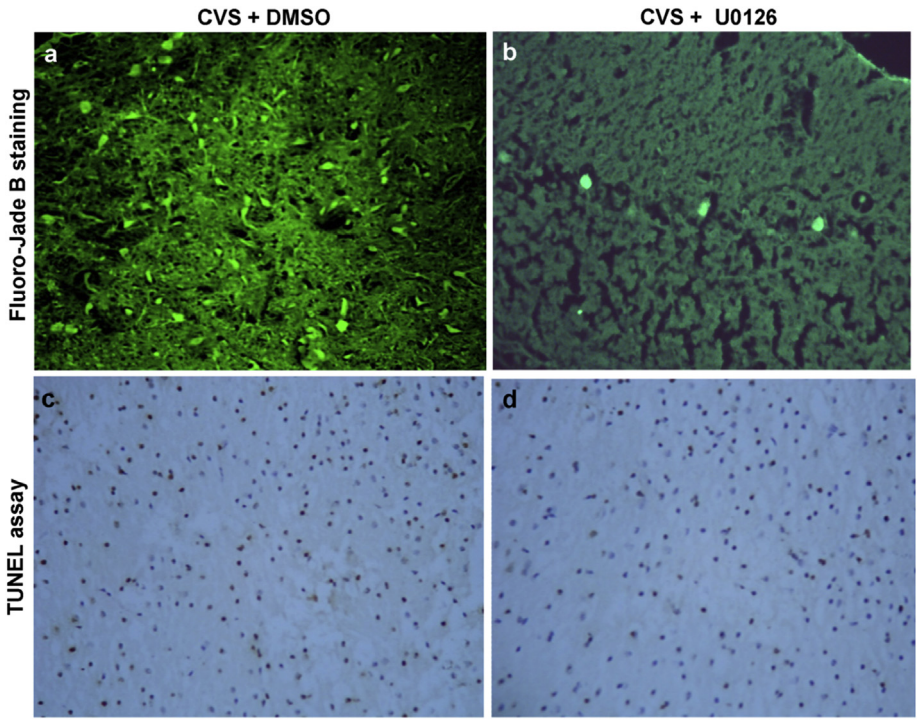

Fig. 9. Fluoro-Jade B staining and TUNEL assay in CVS-infected/mock-treated (a, c) and MEK-ERK1/2 inhibited (b, d) groups. **a.** Brain showing more FJB positive degenerating neurons. x100. **b.** Few FJB positive degenerating neurons in brain. x100. **c.** Brain showing brown colour more TUNEL positive apoptotic cells. x100. **d.** Brain showing few TUNEL positive apoptotic cells. x100. (For interpretation of the references to colour in this figure legend, the reader is referred to the web version of this article.)

reduced viral load and its spread in the brain, as confirmed by qRT-PCR, dFAT and IHC. The results were similar as seen in other viral infections [10,14,16,25]. Treatment with MAPK inhibitor during dengue [28] and avian influenza virus infections in mice [10] resulted in significantly increased survival time.

In CVS-infected/mock-treated group, maximum mortality was observed on 8 and 9 DPI but at the same time, in CVS-infected/U0126-treated group just mortality was started. This might be due to increased ERK levels, viral load and cytokine expressions on 8 and 9 DPI. The CVS-infected/mock-treated group also showed prominent histopathological lesions in brain with more FJB positive degenerating neurons, clearly suggesting the virus-mediated inflammatory and degenerative changes. The infection had proliferating effect on microglial cells and augmenting expressions of iNOS, TNF-α and CXCL10 mRNA levels in the brain, facilitating higher chemotaxis for macrophages/microglial cells, which in turn secreted higher inflammatory cytokines leading to severe histopathological changes. These effects inducing proliferation of microglial cells could be due to ERK 1/2 mediated signalling pathway owing to its mitogenic role [4]. Consistently, treatment with ERK1/2 inhibitor (U0126) reduced all these effects indicating that ERK1/2 mediated viral-induced inflammatory changes and pathologies. Inhibition of MEK-ERK1/2 resulted in less severe lesions in brain, decreased viral load, decreased expressions of CXCL10, TNF-α and iNOS, and reduced proliferation of microglial cells. The inhibitory effects of MEK-ERK1/2 on rabies infection and inflammatory cytokines were reported *in vitro* by Nakamichi et al. [11,12]. Thus, these data emphasize that MEK-ERK1/2 pathway play important role in pathogenesis of rabies.

In the present study, highest levels of ERK have been observed on 5–9 DPI, might be due to increased viral load, which stimulates ERK1/2 signalling pathways. Nakamichi et al. [12] demonstrated that RV infection and replication, but not exposure to inactivated virions, directly activates MAPK-ERK1/2-mediated signalling pathway in microglia. In the present study, CVS-infected/U0126-treated mice had significantly reduced viral loads measured by qRT-PCR and reduced positive signals in dFAT and IHC. It is well proven that MAPK signalling pathway is essential for infection, replication and viral spread, and inhibition leads to defect in replication of many human viral infections viz. HIV-1, HSV-1, rabies virus, PRRSV, Coxsackievirus B3 and others [6–12]. MEK inhibitor U0126 exerts antiviral effect directly in reducing viral load by inactivating virus or indirectly by immunomodulation [14,29]. MEK inhibition also leads to blockade of nuclear cytoplasmic transport of viral ribonucleoproteins (RNPs) complexes [30]. Droebner et al. [14] reported that U0126 treatment against highly pathogenic avian influenza virus and pandemic H1N1v resulted in both *in vitro* and *in vivo* antiviral action. *In vivo* results showed that treatment with U0126 in adult BALB/c mice infected with yellow fever virus significantly reduced the virus titres in brain [16].

In the present study, CVS-infected/mock-treated group showed significantly increased serum NO levels and higher iNOS mRNA levels in brain, as reported previously [18,19]. MAPK/ERK1/2 signalling pathway mediated NO production from macrophages/microglial cells. ERK activates IRF3 stimulating NO-inducing cytokines such as IFN-β, IL-6 and iNOS leading to production of NO [11,31]. During rabies virus infection, it was shown that excess NO induces damage to blood brain barrier (BBB) and neurotoxicity leading to neurodegeneration [18,19,25]. In the present study, increased NO level was correlated positively with prominent histopathological lesions in brain. In addition, a positive correlation was seen between NO, CXCL10 and TNF-α concentrations with brain lesions.

On the other hand, the CVS-infected/U0126-treated mice reacted less severely to infection which correlated with decreased serum NO and iNOS mRNA levels in brain, with perceptible decrease in clinical signs and mortality. Nakamichi et al. [11] reported that *in vitro* MAPK/ERK kinase inhibition resulted in

significantly decreased NO production from rabies virus infected macrophages. Decreased/inhibition of NO by iNOS inhibitor significantly increased the survival time of mice and delay in development of clinical signs during rabies virus infection [18,19].

Even though ERK1/2 is a pro-survival factor in the MAP kinase family and contributes to the regulation of cell proliferation and differentiation, under some circumstances, ERK1/2 can function in a pro-apoptotic manner. In the neuronal system, ERK1/2 has been suggested to be involved in neurodegeneration [32] and ERK1/2 activation promotes low potassium-induced neuronal degeneration predominantly through caspase-3 dependent plasma membrane damage [33]. In the present study, neurodegenerative lesions of brain were observed in the infected mice with increased expression of caspase-3 and TNF-α, but a significant decrease in Bcl-2 mRNA levels. Further, greater number of TUNEL positive apoptotic cells with typical DNA ladder pattern was observed, suggesting ERK-mediated cell death. MAPK signalling pathways play an important role in the initiation and progression of cell death [34]. MAPK family members like ERK pathways are activated during viral infection, and communicate apoptotic signals within cells [4,5,35]. TNF-α also mediates apoptosis during virus infection via activation of Ras/Raf/ERK signalling pathways inducing phosphorylation of Bcl-2 leading to cytochrome *c* release and caspase-3 activation in mitochondria [36]. MAPK pathway mediated apoptosis is unique during viral infections like bluetongue virus, alphaherpesvirus, reovirus and Japanese encephalitis virus [24,32,37]. Inhibition of MEK-ERK1/2 pathway also confers protection against neuronal cell death by reducing Bax expression, mitochondrial membrane depolarization, cytochrome *c* release, caspase-3 activation and ultimately lead to inhibition of apoptosis [13,37,38]. Thus, ERK inhibitor treatment reduced dead cells in CVS-infected mice.

Migrating T lymphocytes from the periphery through BBB provides protection against infections in brain [39]. In CVS-infected/mock-treated mice early increase and thereafter significant decrease in $CD4^+$, $CD8^+$ T cells and NK cells in blood and spleen was remarkable. During rabies virus infection $CD8^+$ T lymphocytes become ineffective due to apoptosis of migrating T cells. Also rabies virus infected neurons did not reveal apoptosis but leukocytes became apoptotic [1,2,40]. Presently, increase in caspase-3 and TNF-α, and decrease in Bcl-2 in brain appeared to be responsible for apoptosis of T and NK cells. Rabies virus increases the expression of various pro-apoptotic and other genes in both the infected and non-infected neurons as well as non-neuronal resident cells of CNS [41,42]. The morphology of TUNEL positive apoptotic cells confirmed that lymphocytes were undergoing apoptosis. In our study, ERK inhibitor reduced TNF-α expression with ameliorating brain lesions and less T cell death suggesting that MEK/ERK-dependent TNF-α play a role in apoptosis of T cells.

The present study reported for the first time that MEK-ERK1/2 inhibition *in vivo* had protected T cells from demise during rabies infection. It could be due to reduced rabies viral load in brain resulting in reduced killing of protective migrating T cells. MEK-ERK1/2 inhibition during rabies infection exhibited anti-apoptotic effect on T cells with decreased clinical expression of disease and low mortality.

In conclusion, CVS-infected/mock-treated mice developed severe histopathological lesions and FJB positive degenerating neurons along with increased serum NO, CXCL10, iNOS, TNF-α, and caspase 3 mRNA levels. Treatment with specific inhibitor of MEK1/2, U0126 had clinically and pathologically deterred the intensity clinical expressions, morbidity and mortality in rabies virus infection in mice. The present study for the first time evidenced the role of MEK-ERK1/2 signalling pathway in the pathogenesis of rabies virus infection *in vivo*. Further studies using mice with gene knockout for MEK-ERK/MAPK pathway would reveal the critical role these molecules for pathogenesis of rabies.

Acknowledgement

The authors thank the Director, Joint Directors and Head, Division of Pathology, ICAR-Indian Veterinary Research Institute, Izatnagar for the facilities provided during the study. The financial assistance in the form of Junior Research Fellowship (JRF) to first author provided by Indian Council of Agricultural Research (Roll no.: 020691), New Delhi is duly acknowledged.

References

[1] M. Lafon, Immune evasion, a critical strategy for rabies virus, Dev. Biol. 131 (2008) 413–419.
[2] M. Lafon, Evasive strategies in rabies virus infection, in: A.C. Jackson (Ed.), Advances in Virus Research, Academic Press, Burlington, MA, 2011, p. 3355.
[3] R. Singh, K.P. Singh, S. Cherian, M. Saminathan, S. Kapoor, G.B. Manjunatha Reddy, S. Panda, K. Dhama, Rabies - epidemiology, pathogenesis, public health concerns and advances in diagnosis and control: a comprehensive review, Vet. Q. 37 (2017) 212–251.
[4] Z. Lu, S. Xu, ERK1/2 MAP kinases in cell survival and apoptosis, IUBMB Life 58 (2006) 621–631.
[5] S. Cagnol, J.C. Chambard, ERK and cell death: mechanisms of ERK-induced cell death-apoptosis, autophagy and senescence, FEBS J. 277 (2010) 2–21.
[6] O. Planz, S. Pleschka, S. Ludwig, MEK-specific inhibitor U0126 blocks spread of Borna disease virus in cultured cells, J. Virol. 75 (2001) 4871–4877.
[7] H. Luo, B. Yanagawa, J. Zhang, Z. Luo, M. Zhang, M. Esfandiarei, et al., Coxsackievirus B3 replication is reduced by inhibition of the extracellular signal-regulated kinase (ERK) signalling pathway, J. Virol. 76 (2002) 3365–3373.
[8] S. Ludwig, T. Wolff, C. Ehrhardt, W.J. Wurzer, J. Reinhardt, O. Planz, et al., MEK inhibition impairs influenza B virus propagation without emergence of resistant variants, FEBS Lett. 561 (2004) 37–43.
[9] L.A. Moser, S. Schultz-Cherry, Suppression of Astrovirus replication by an ERK1/2 inhibitor, J. Virol. 82 (2008) 7475–7482.
[10] Y. Börgeling, M. Schmolke, D. Viemann, C. Nordhoff, J. Roth, S. Ludwig, Inhibition of p38 mitogen-activated protein kinase impairs influenza virus-induced primary and secondary host gene responses and protects mice from lethal H5N1 infection, J. Biol. Chem. 289 (2014) 13–27.
[11] K. Nakamichi, S. Inoue, T. Takasaki, K. Morimoto, I. Kurane, Rabies virus stimulates nitric oxide production and CXC chemokine ligand10 expression in macrophages through activation of extracellular signal regulated kinases 1 and 2, J. Virol. 78 (2004) 9376–9388.
[12] K. Nakamichi, M. Saiki, M. Sawada, M. Takayama, Y. Yamamuro, K. Morimoto, et al., Rabies virus-induced activation of mitogen-activated protein kinase and NF-κB signalling pathways regulates expression of CXC and CC chemokine ligands in microglia, J. Virol. 79 (2005) 11801–11812.
[13] S.K. Jo, W.Y. Cho, S.A. Sung, H.K. Kim, N.H. Won, MEK inhibitor, U0126, attenuates cisplatin-induced renal injury by decreasing inflammation and apoptosis, Kidney Int. 67 (2005) 458–466.
[14] K. Droebner, S. Pleschka, S. Ludwig, O. Planz, Antiviral activity of the MEK-inhibitor U0126 against pandemic H1N1v and highly pathogenic avian influenza virus *in vitro* and *in vivo*, Antivir. Res. 92 (2011) 195–203.
[15] M.E. Rodríguez, J.E. Brunetti, M.B. Wachsman, L.A. Scolaro, V. Castilla, Raf/MEK/ERK pathway activation is required for Junín virus replication, J. Gen. Virol. 95 (2014) 799–805.
[16] J.D. Albarnaz, L.C. De Oliveira, A.A. Torres, R.M. Palhares, M.C. Casteluber, C.M. Rodrigues, et al., MEK/ERK activation plays a decisive role in yellow fever virus replication: implication as an antiviral therapeutic target, Antivir. Res. 111 (2014) 82–92.
[17] T.L. Sorensen, C. Trebst, P. Kivisakk, K.L. Klaege, A. Majmudar, R. Ravid, et al., Multiple sclerosis: a study of CXCL10 and CXCR3 co-localization in the inflamed central nervous system, J. Neuroimmunol. 127 (2002) 59–68.
[18] S. Ubol, C. Sukwattanapan, Y. Maneerat, Inducible nitric oxide synthase inhibition delays death of rabies virus-infected mice, J. Med. Microbiol. 50 (2001) 238–242.
[19] B.P. Madhu, K.P. Singh, M. Saminathan, R. Singh, A.K. Tiwari, V. Manjunatha, et al., Correlation of inducible nitric oxide synthase (iNOS) inhibition with TNF-α, caspase-1, FasL and TLR-3 in pathogenesis of rabies in mouse model, Virus Genes 52 (2016) 61–70.
[20] T.J. Haley, W.G. McCormick, Pharmacological effects produced by intracerebral injection of drugs in the conscious mouse, Br. J. Pharmacol. Chemother. 12 (1957) 12–15.
[21] L. Baloul, S. Camelo, M. Lafon, Up-regulation of Fas ligand (FasL) in the central nervous system: a mechanism of immune evasion by rabies virus, J. Neurovirol 10 (2004) 372–382.
[22] O.H. Lowry, N.J. Rosebrough, A.L. Farr, R.J. Randall, Protein measurement with the Folin phenol reagent, J. Biol. Chem. 193 (1951) 265–275.
[23] C.S. McKimmie, N. Johnson, A.R. Fooks, J.K. Fazakerley, Viruses selectively

upregulate Toll-like receptors in the central nervous system, Biochem. Biophys. Res. Commun. 336 (2005) 925–933.
[24] M.L. Nagpal, Y. Chen, T. Lin, Effects of overexpression of CXCL10 (cytokine-responsive gene-2) on MA-10 mouse Leydig tumor cell steroidogenesis and proliferation, J. Endocrinol. 183 (2004) 585–594.
[25] S.Q. Doi, T.A. Jacot, D.F. Sellitti, P. Hirszel, M.H. Hirata, G.E. Striker, et al., Growth hormone increases inducible nitric oxide synthase expression in mesangial cells, J. Am. Soc. Nephrol. 11 (2000) 1419–1425.
[26] S. Shams, S. Mohsin, G.A. Nasir, M. Khan, S.N. Khan, Mesenchymal stem cells pretreated with HGF and FGF4 can reduce liver fibrosis in mice, Stem Cells Int. (2015) 747245.
[27] L.C. Schmued, K.J. Hopkins, B. Fluoro-Jade, A high affinity fluorescent marker for the localization of neuronal degeneration, Brain Res. 874 (2000) 123–130.
[28] Y. Fu, A. Yip, P.G. Seah, F. Blasco, P.Y. Shi, M. Hervé, Modulation of inflammation and pathology during dengue virus infection by p38 MAPK inhibitor SB203580, Antivir. Res. 110 (2014) 151–157.
[29] T. Nakayama, M. Yamashita, The TCR-mediated signalling pathways that control the direction of helper T cell differentiation, Semin. Immunol. 22 (2010) 303–309.
[30] S. Pleschka, T. Wolff, C. Ehrhardt, G. Hobom, O. Planz, U.R. Rapp, S. Ludwig, Influenza virus propagation is impaired by inhibition of the Raf/MEK/ERK signalling cascade, Nat. Cell Biol. 3 (2001) 301–305.
[31] T.C. Moore, T.M. Petro, IRF3 and ERK MAP-kinases control nitric oxide production from macrophages in response to poly-I: C, FEBS Lett. 587 (2013) 3014–3020.
[32] E.C. Cheung, R.S. Slack, Emerging role for ERK as a key regulator of neuronal apoptosis, Sci. STKE 2004 (2004) PE45.
[33] S. Subramaniam, U. Zirrgiebel, O. von Bohlen Und Halbach, J. Strelau, C. Laliberte, D.R. Kaplan, et al., ERK activation promotes neuronal degeneration predominantly through plasma membrane damage and independently of caspase-3, J. Cell Biol. 165 (2004) 357–369.
[34] E. Mortola, A. Larsen, Bluetongue virus infection: activation of the MAP kinase-dependent pathway is required for apoptosis, Res. Vet. Sci. 89 (2010) 460–464.
[35] S. Subramaniam, K. Unsicker, ERK and cell death: ERK1/2 in neuronal death, FEBS J. 277 (2010) 22–29.
[36] C.J. Yeh, P.Y. Lin, M.H. Liao, H.J. Liu, J.W. Lee, S.J. Chiu, et al., TNF-alpha mediates pseudorabies virus-induced apoptosis via the activation of p38 MAPK and JNK/SAPK signalling, Virology 381 (2008) 55–66.
[37] D.C. Hooper, S.T. Ohnishi, R. Kean, Y. Numagami, B. Dietzschold, H. Koprowski, Local nitric oxide production in viral and autoimmune diseases of the central nervous system, Proc. Natl. Acad. Sci. U. S. A. 92 (1995) 5312–5316.
[38] S. Schweyer, A. Soruri, O. Meschter, A. Heintze, F. Zschunke, N. Miosge, et al., Cisplatin-induced apoptosis in human malignant testicular germ cell lines depends on MEK/ERK activation, Br. J. Cancer 91 (2004) 589–598.
[39] B.P. Madhu, K.P. Singh, M. Saminathan, R. Singh, N. Shivasharanappa, A.K. Sharma, et al., Role of nitric oxide in the regulation of immune responses during rabies virus infection in mice, VirusDis 27 (2016) 387–399.
[40] M. Lafon, Modulation of the immune response in the nervous system by rabies virus, Curr. Top. Microbiol. Immunol. 289 (2005) 239–258.
[41] M. Prosniak, D.C. Hooper, B. Dietzschold, H. Koprowski, Effect of rabies virus infection on gene expression in mouse brain, Proc. Natl. Acad. Sci. U. S. A. 98 (2001) 2758–2763.
[42] S. Ubol, J. Kasisith, C. Mitmoonpitak, D. Pitidhamabhorn, Screening of upregulated genes in suckling mouse central nervous system during the disease stage of rabies virus infection, Microbiol. Immunol. 50 (2006) 951–959.